

Density-dependent potential for multi-neutron halo nuclei*

CHEN Shuang(陈双)^{1,3;1)} CHU Yan-Yun(褚衍运)^{1,3} REN Zhong-Zhou(任中洲)^{1,2,3}

1 (Department of Physics, Nanjing University, Nanjing 210008, China)

2 (Center of Theoretical Nuclear Physics, National Laboratory of Heavy-Ion Accelerator at Lanzhou, Lanzhou 730000, China)

3 (Joint Center for Particle, Nuclear Physics and Cosmology, Nanjing 210008, China)

Abstract We apply a simple density-dependent potential model to the three-body calculation of the ground-state structure of drip-line nuclei with a weakly bound core. The hyperspherical harmonics method is used to solve the Faddeev equations. There are no undetermined potential parameters in this calculation. We find that for the halo nuclei with a weakly-bound core, the calculated properties of the ground-state structure are in better agreement with experimental data than the results calculated from the standard Woods-Saxon and Gauss type potentials. We also successfully reproduce the experimental cross sections by using the density calculated from this method. This may be explained by the fact that the simple Fermi or Gaussian function can not exactly describe the density distribution of the drip-line nuclei.

Key words density-dependent, three-body model, halo nuclei

PACS 21.10.Dr, 21.60.Gx, 27.20.+n

1 Introduction

The extremely diluted matter distribution of drip-line nuclei has been an attractive topic in nuclear physics for a couple of decades^[1]. The few-body models for weakly bound neutron halo nuclei have been well established during these years^[2–15]. Various methods have been used in these models: the variational approach^[2, 3], the cluster-orbital shell model^[4], the two-particle Green's function method^[5], the variational shell model^[6], the coordinate space Faddeev approach, and the hyperspherical harmonics method^[7].

A basic assumption of this few-body cluster picture is that the core is inserted with frozen intrinsic freedom. But this point may be invalid when the core is considerably coupled with low excited states or not bound tightly enough. A few-body model with core excitation is now being developed^[8, 9]. For the latter condition, we may face more complicate few-body models by redefining a core. For instance, ${}^6\text{He}$ can be

well described by an $\alpha+n+n$ model^[10], but one can hardly describe ${}^8\text{He}$ by a ${}^6\text{He}+n+n$ model with the phenomenological core-N interactions. One can solve a model of α plus four neutrons for ${}^8\text{He}$ ^[16], but it is unpractical for us to study the halo nuclei by solving the five or even more body problem because of the mathematical difficulty and complication.

The main input values in the few-body calculation are the interaction parameters. In the three-body model, a pertinent question is whether the phenomenological interactions, such as the Woods-Saxon type potential, apply to the drip-line nuclei in which the core nucleus itself may be weakly bound. The extremely diluted matter distribution is the characteristic of the halo nuclei. The effective interactions in the weakly bound nuclei may be correlated with the matter density. We know that the density-dependent effective interactions have been successfully applied to the nucleus-nucleus scattering^[17–19] and the cluster structure in nuclei^[20–26]. It may be appropriate to bring this type of potential into the calculation of

Received 2 December 2008

* Supported by National Natural Science Foundation of China (10535010, 10675090, 10775068), 973 National Major State Basic Research and Development of China (2007CB815004), CAS Knowledge Innovation Project (KJCX2-SW-N02) and Research Fund of Doctoral Point (20070284016)

1) E-mail: shuangphy@gmail.com

©2009 Chinese Physical Society and the Institute of High Energy Physics of the Chinese Academy of Sciences and the Institute of Modern Physics of the Chinese Academy of Sciences and IOP Publishing Ltd

the structure of halo nuclei. In this work we try to apply the density-dependent potential in the three-body model for halo nuclei in which the core nuclei are weakly bound. We test our method by comparing the results with the experimental structure and reaction data. As the experimental root-mean-square (rms) radius is always deduced by the reaction cross section measurements^[27–30], in this work we also try to discuss the effect of the diffused density distribution on the reaction calculation.

In the next section, we present the potential model used in our calculations and the results of these calculations are presented in Sect. 3. In Sect. 4 we discuss the effect of the density function on the reaction calculation. Sect. 5 is devoted to our summary and conclusion.

2 Density-dependent potential for a weakly bound core

The three-body Hamiltonian for the core+N+N system is

$$H = \sum_{i=1}^3 T_i - T_G + V_{nc}(r_1) + V_{nc}(r_2) + V_{nn}(r_3), \quad (1)$$

where T_i , T_G are the kinetic operator for the i th particle and center of mass. V_{nc} and V_{nn} are the core-N and NN potential, respectively. We consider the central and spin-orbit interactions for V_{nc}

$$V_{nc}(r) = V_c(r) + V_{so}(r). \quad (2)$$

The spin-orbit part is taken to be

$$V_{so}(r) = -V_{so} \frac{1}{r} \left| \frac{dV_c(r)}{dr} \right| \mathbf{l} \cdot \mathbf{s}. \quad (3)$$

A density-dependent potential with no deformation for the central part of core-N interaction can be written as

$$V_c(r) = \int d\mathbf{r}' \rho(r') v_{nn}(|\mathbf{r} - \mathbf{r}'|), \quad (4)$$

where r is the core-N distance (Fig. 1). v_{nn} is the effective NN potential.

Here we assume that the core nucleus has a weakly bound structure. The density distribution of the core nucleus ρ can be divided into two parts

$$\rho(r) = \rho_c(r) + \rho_v(r), \quad (5)$$

where $\int \rho_c(r) d\mathbf{r} = A_c$, $\int \rho_v(r) d\mathbf{r} = A_v$, and $A_c + A_v = A$. A is the mass number of the core nucleus. The label c represents the stable part of the core nucleus, and v represents the valence nucleon(s). The rms matter

radius satisfies the relation^[31].

$$r_A^2 = \frac{A_c}{A} \left(r_c^2 + \frac{A_v}{A} r_v^2 \right), \quad (6)$$

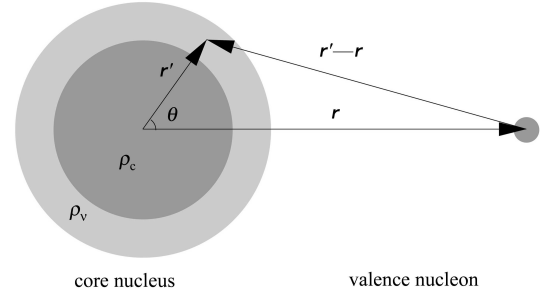


Fig. 1. Schematic explanation of coordinates used in the density-dependent potential (without deformation) for the core-N system with a weakly bound core.

After determining the Hamiltonian, we solve the Faddeev equations

$$(T_i - E)\Psi_i + \sum_{i=1}^3 V_i \Psi = 0 \quad (i = 1, 2, 3), \quad (7)$$

where $\Psi = \Psi_1 + \Psi_2 + \Psi_3$ is the total wave function. These equations can be efficiently solved by the hyperspherical expansion method for short-range interactions^[11]. V_i ($i=1, 2, 3$) are the two-body potentials described above. In the three-body cluster picture, one can calculate the matter radius by^[10]

$$r_{A+2}^2 = \frac{A}{A+2} r_A^2 + \frac{1}{A+2} \langle \rho^2 \rangle, \quad (8)$$

where ρ is the hyper-radius. Using the hyperspherical expansion, one can convert the two-dimensional partial differential equations (Eq. (7)) into a set of coupled one-dimensional equations

$$\frac{\hbar^2}{2m} \left[-\frac{d^2}{d\rho^2} + \frac{(K_i + 3/2)(K_i + 5/2)}{\rho^2} - \frac{2mE}{\hbar^2} \right] \times \chi_{\Omega_i K_i}^i(\rho) + \sum_{j \Omega_j K_j} V_{\Omega_i K_i, \Omega_j K_j}^{ij}(\rho) \chi_{\Omega_j K_j}^j(\rho) = 0, \quad (9)$$

where

$$V_{\Omega_i K_i, \Omega_j K_j}^{ij}(\rho) = \langle \varphi_{j, K_j}^{l_{xj} l_{yj}}(\theta_j) | V_{ij} | \varphi_{i, K_i}^{l_{xi} l_{yi}}(\theta_i) \rangle$$

is the hyper-angular integration of the two-body interaction. Here $\Omega_i \equiv \{(l_{xi}, l_{yi})L_i, (s_j, s_k)S_{xi}\}J_i$. K_i is the hyper-angular-momentum. The indexes i, j, k run through (1, 2, 3) in circular order for three sets of Jacobi coordinates. The Laguerre polynomial expansion is used to solve these coupled equations^[32]. In order to eliminate the two-body forbidden states, the supersymmetric transformations^[33] can be used for the two-body potentials. Then the remaining work is

calculating the potential matrix elements and finding the eigenvalues for a generalized eigenvalue problem.

An important advantage of this density-dependent potential for the three-body model is that all of the potential parameters can be determined before calculation. The shape of the potential is well determined by the density distribution and the effective NN interaction, and the potential strength is determined by the experimental data of the properties of the core-N subsystem.

3 Three-body calculation

For simplicity, we apply this method to ${}^8\text{He}$. The δ -force and M3Y^[34–38] type NN interactions are considered in the following calculation. The δ -force is

$$v_{nn}(r) = \bar{\alpha}\delta(r) \text{ MeV}. \quad (10)$$

This zero-range approximation has been successfully used in the study of the cluster structure of nuclei^[13, 17]. The M3Y type NN effective interaction is used in the form^[35, 36]

$$v_{nn}(r) = Fv(r), \quad (11)$$

where r is the internucleon separation, and F is the potential strength parameter. The radial shape of the M3Y interaction used in the present calculation is given in terms of Yukawa form^[37]

$$v(r) = 7999 \frac{\exp(-4r)}{4r} - 2134 \frac{\exp(-2.5r)}{2.5r} - 276\delta(r). \quad (12)$$

There is no energy-dependent term in this form. Here the density dependence $F(\rho)$ and the strength parameter $\bar{\alpha}$ are determined by the properties of the the core-N system.

We choose $A_c = 4$, $A_v = 2$ for the core nucleus ${}^6\text{He}$. The α density is selected as^[38]

$$\rho_c(r) = \frac{4}{\pi^{3/2}b_\alpha^3} \exp\left(-\frac{r^2}{b_\alpha^2}\right), \quad (13)$$

with $b_\alpha = 1.1932$. The rms radius of ${}^4\text{He}$ is 1.57 fm according to this density. Then we obtain ρ_v from the well-established three-body calculation for ${}^6\text{He}$ ^[10, 13]. This numerically calculated density and the α density are shown in Fig. 2.

ρ_v is numerically calculated from the well established three-body model^[10, 13]. $4\pi \int r^2 \rho_c(r) dr = 4.0$; $4\pi \int r^2 \rho_v(r) dr = 2.0$; $r_c = 1.57$ fm, $r_v = 4.53$ fm. $r = 2.49$ fm according to Eq. (6). The experimental rms matter radiuses of ${}^4\text{He}$ and ${}^6\text{He}$ are (1.57 ± 0.04) fm and (2.48 ± 0.03) fm, respectively^[39].

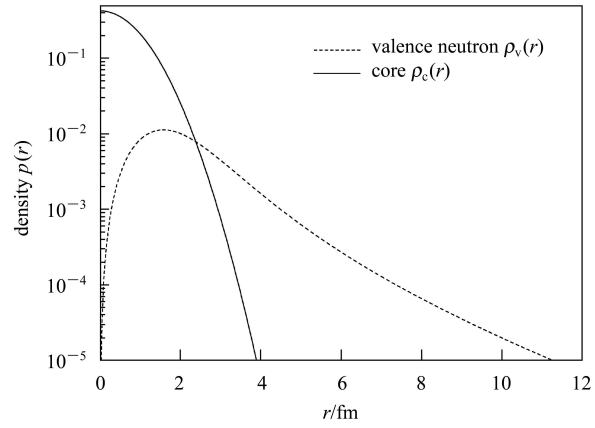


Fig. 2. Density distribution of ${}^6\text{He}$.

The Woods-Saxon and Gauss type potentials with standard parameters are also considered for comparison. The core-n potentials used in our calculation are numerically shown in Fig. 3 and Fig. 4. All these single particle potentials approximately reproduce the bound $3/2^-$ (-0.43 MeV) state of ${}^7\text{He}$. And the $1/2^+$

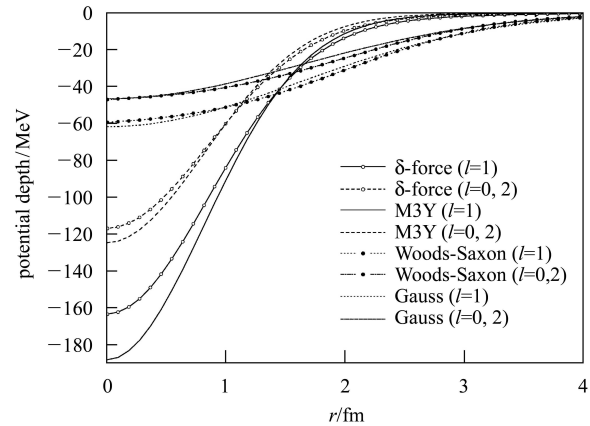


Fig. 3. The central part of the core-n potential used in the three-body calculation.

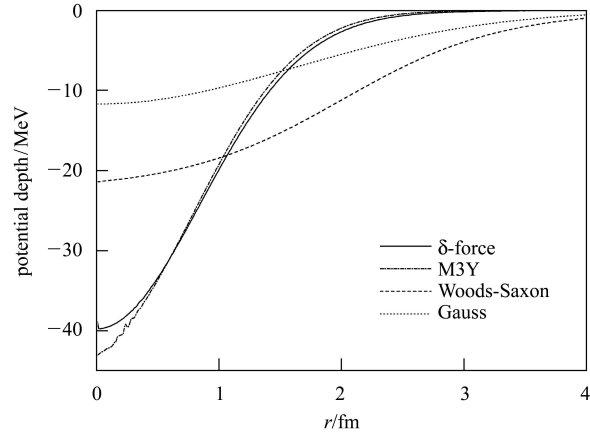


Fig. 4. The spin-orbit potentials used in the three-body calculation. $V_{so} = 5.57$ MeV for the folded potential.

state is bound by 20.58 MeV (the one neutron separation energy of ${}^4\text{He}$) which is eliminated by supersymmetric transformations^[32]. The NN potential parameters are $\bar{\sigma}=22.01$, $F=0.68$ for $l=0, 2$ and $\bar{\sigma}=33.06$, $F=0.46$ for $l=1$. The corresponding spin-orbit potential is shown in Fig. 4. The potential parameters which are determined by the experimental data of ${}^7\text{He}$ are given in the corresponding text. As we can see, the range of standard Woods-Saxon or Gauss type potentials is larger than the density-dependent ones. As the density function dominates the integral in Eq. (4) at the long range part by the rapidly disappearing term $\exp(-r^2/a^2)$, there is little difference between the two shapes of the potentials calculated from the zero range and M3Y type NN interactions.

The main results are listed in Table 1. All the

core-n potentials are determined by reproducing the ground-state properties of ${}^7\text{He}$. The calculated density distribution of the last two halo neutrons (ρ_h) and the total density of ${}^6\text{He}$ ($\rho_c + \rho_v$) used in the calculation are shown in Fig. 5. r_h (3.09 fm) is less than r_v (4.53 fm). For Woods-Saxon and Gauss type potentials, r_h is 3.86 fm and 3.97 fm, respectively. As we can see, the density-dependent potential integrated from the zero range or M3Y type NN interaction can give fairly good results compared with Woods-Saxon and Gauss type potentials (Table 1). In fact, as the simple Fermi or Gaussian function can not exactly describe the density distribution of the drip-line nuclei, the phenomenological Woods-Saxon or Gauss type potentials should be modified for the weakly bound nuclei.

Table 1. The results of the three-body calculation for ${}^8\text{He}$. DD represents the density-dependent potential. ρ is the hyper-radius. Woods-Saxon parameters are $r_0 = 1.2 \times 6^{1/3}$ fm, $a = 0.65$ fm. The potential range of the Gauss type potential is 2.30 fm. V_{nn} is in the GPT form Ref. [40] for all cases. The core-n potentials used in these calculations are shown in Fig. 3 and Fig. 4. Energy and length are given in units of MeV and fm, respectively.

	DD (δ -force)	DD(M3Y)	Woods-Saxon	Gauss	Exp.
S_{2n}	2.14	2.10	2.16	2.04	2.140 ± 0.007 ^[41]
rms	2.53	2.51	2.75	2.77	2.52 ± 0.03 ^[39]
$\langle \rho \rangle$	3.81	3.69	4.85	4.92	

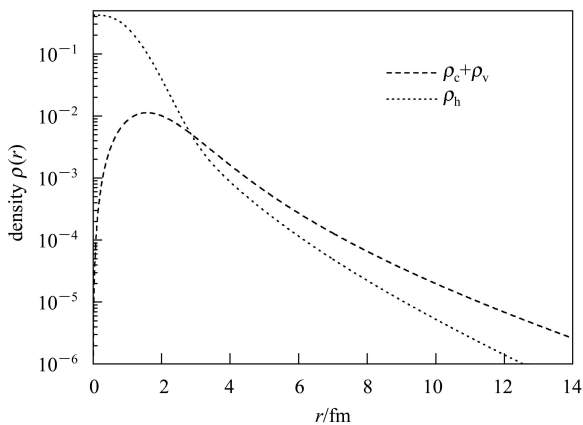


Fig. 5. The density distribution of ${}^8\text{He}$. ρ_h is the results of the three-body calculation with folded core-n potential. $4\pi \int r^2 \rho_h(r) dr = 2.0$. $r_h = 3.09$ fm. The total rms radius is $r_m = 2.53$ fm.

From this simple example, we find that the density-dependent potential used in the three-body model can give a result which is in good agreement with the halo structure of ${}^8\text{He}$. More calculations can be carried out for other drip-line nuclei using this method.

4 Reaction calculation

The matter rms radiuses of short-lived exotic nuclei have been extensively studied by reaction cross section measurements^[27–30]. The Glauber model^[42–46], which is based on the assumed static matter distribution of nuclei, is an important method for deducing the rms radius from reaction data^[29, 47].

In the Glauber model, the total reaction cross section is written as

$$\sigma_R = 2\pi \int_0^\infty [1 - T(b)] b db, \quad (14)$$

where $T(b)$ is the transparency function at impact parameter b . Assuming the optical limit approximation with zero-range nuclear interaction, one has

$$T(b) = \exp[-\bar{\sigma}_{NN} \int ds \bar{\rho}_T(s) \bar{\rho}_P(|b-s|)], \quad (15)$$

where $\bar{\rho}_i(s)$ are the thickness functions^[45]. For the projectile, we have $\rho_P(r) = \rho_c(r) + \rho_v(r)$, $T(b) = T_c(b)T_v(b)$. The average NN cross section $\bar{\sigma}_{NN}$ and the static density distributions of both the target ($\rho_T(r)$) and the projectile ($\rho_P(r)$) are needed to compute the total reaction cross section. It has been shown that

this method reproduces the observed cross sections at 400 and 800 AMeV within 2% for all reactions involving ${}^7\text{Li}$, ${}^9\text{Be}$, ${}^{12}\text{C}$, and ${}^{27}\text{Al}$ ^[47]. So this simple optical-limit Glauber model has been proved to work well at relatively high energies^[47]. As the recent experimental data are available^[48], we study the effects of the matter density of ${}^{6,8}\text{He}$ on the ${}^1\text{H}({}^6\text{He}, {}^6\text{He})$ and ${}^1\text{H}({}^8\text{He}, {}^8\text{He})$ reaction calculation at an energy near 700 AMeV.

We consider four types of mass density for ${}^{6,8}\text{He}$: 1. The numerically obtained density from the above calculation. We abbreviate it as FB type density in the following text. 2. The Gaussian core density with a diffused tail^[49]

$$\rho(r) = \frac{1}{\pi^{3/2}} \left[\frac{4}{b_c^3} \exp\left(-\frac{r^2}{b_c^2}\right) + \frac{N-2}{b_v^3} \frac{r^2}{a_v^3} \exp\left(-\frac{r^2}{a_v^2}\right) \right]. \quad (16)$$

Table 2. Parameters of density function used in the present study. All the densities are obtained by the same rms radius of ${}^{6,8}\text{He}$.

	Tail			Gauss		Fermi	
	b_c/fm	b_v/fm	a_v/fm	ρ_0^G/fm^{-3}	a_0/fm	ρ_0^F/fm^{-3}	a/fm
${}^6\text{He}$	1.193	2.300	2.848	0.130	2.025	0.118	1.883
${}^8\text{He}$	1.193	1.771	1.925	0.165	2.058	0.143	1.969

It is denoted as Tail type density in the following text. 3. The simple Gaussian density

$$\rho(r) = \rho_0^G \exp(-r^2/a_0^2). \quad (17)$$

4. The usually used Fermi type density

$$\rho(r) = \frac{\rho_0^F}{1 + \exp\left[\frac{r - R_0}{a}\right]}, \quad (18)$$

where the diffuseness parameter $a = 0.54$ fm is taken from Ref. [50]. The other parameters are determined by the experimental matter rms radius and integrat-

ing the density distribution equivalent to the mass number of the corresponding nucleus (Table 2).

The results of the reaction calculation are shown in Table 3. We can see that the cross sections data can be well reproduced by the FB density. So our few-body calculation can be supported by this result. Meanwhile, the Gauss and Fermi density can also reproduce the cross sections. The Tail density failed to reproduce $\sigma_R({}^6\text{He}+p)$. It is obvious that the total cross sections are not sensitive to the details of matter density when we fit the densities to the same rms radius.

Table 3. The calculated reaction cross sections near 700 MeV/nucleon using FB, Gauss and Tail type density distributions. The average NN cross section is 43 mb and 42 mb for ${}^6\text{He}+p$ (721 AMeV) and ${}^8\text{He}+p$ (678 AMeV), respectively^[45]. The cross sections are given in unit of mb.

	$\sigma_R(\text{FB})$	$\sigma_R(\text{Tail})$	$\sigma_R(\text{Gauss})$	$\sigma_R(\text{Fermi})$	σ_R^{exp}
${}^6\text{He} + p$ (721 AMeV)	168.2	180.3	170.3	167.1	161.3 ± 3.7 ^[48]
${}^8\text{He} + p$ (678 AMeV)	196.7	202.8	202.2	198.5	197.8 ± 3.5 ^[48]

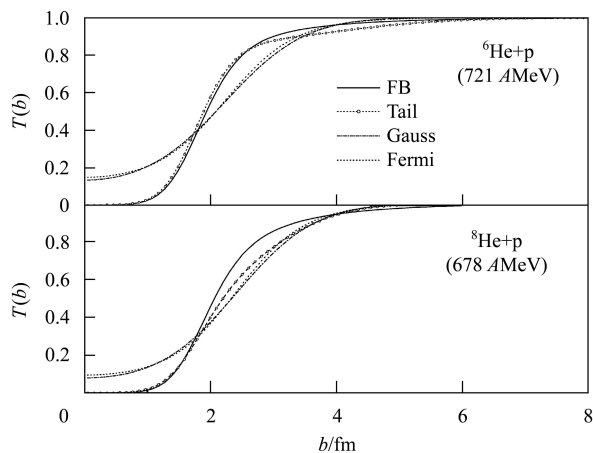


Fig. 6. The transparency function $T(b)$ in the Glauber model calculation.

In Fig. 6 we show the transparency function $T(b)$ in our Glauber model calculation. The transparency function $T(b)$ is more sensitive than the total reaction cross section to the density. The behavior of $T(b)$ calculated from the FB density can only be reproduced by the Tail density at small b . The Gaussian and Fermi densities fail to describe the reaction process, although these two types of density are always used to deduce the rms radius. This may also be explained by the fact that they can not exactly describe the realistic matter distribution of the halo nuclei.

5 Summary

In this work we construct a simple density-

dependent potential model and apply it to calculate the structure of drip-line nuclei (${}^8\text{He}$) in which the core nucleus (${}^6\text{He}$) is weakly bound. We use the three-body model by solving the Faddeev equations. We find that the calculated ground-state properties, especially the matter distribution, are in better agreement with experiment than the results calculated from the Woods-Saxon and Gauss type potentials. We also reproduce the experimental cross sections by using the density calculated from our method. According to our study, the halo density may affect the core-n

(or core-cluster) interactions which are important in the few-body calculation, and it also affects the reaction calculation in the Glauber model which is extensively used for deducing the matter rms radius. This density-dependent potential model can be applied to a wide range of nuclei with different A_c and A_v . For instance, we can calculate ${}^{10}\text{He}$ for $A_c = 4, A_v = 4$ using the calculated density of ${}^8\text{He}$. A double folding potential can be used for the cluster-core or cluster-cluster interaction. Additionally, deformation can also be considered for heavier nuclei.

References

- 1 Tanihata I. *J. Phys. G*, 1996, **22**: 157
- 2 Hansen P G, Jonson B. *Europhys. Lett.*, 1987, **4**: 409
- 3 REN Zhong-Zhou, XU Gong-Ou. *Phys. Lett. B*, 1990, **25**: 311
- 4 Tosaka Y, Suzuki Y. *Nucl. Phys. A*, 1990, **512**: 46
- 5 Bertsch G F, Esbensen H. *Ann. Phys.*, 1991, **209**: 327
- 6 Otsuka T, Fukunishi N, Sagawa H. *Phys. Rev. Lett.*, 1993, **70**: 1385
- 7 Zhukov M V, Danilin B V, Fedorov D V, Bang J M, Thompson I J, Vaagen J S. *Phys. Rep.*, 1993, **231**: 151
- 8 Nunes F M, Christley J A, Thompson I J, Johnson R C, Efos V D. *Nucl. Phys. A*, 1996, **609**: 43
- 9 Nunes F M, Thompson I J, Tostevin J A. *Nucl. Phys. A*, 2002, **703**: 593
- 10 Bang J M, Danilin B V, Efos V D, Vaagen J S, Zhukov M V, Thompson I J. *Phys. Rep.*, 1996, **264**: 27
- 11 Nielsen E, Fedorov D V, Jensen A S, Garrido E. *Phys. Rep.*, 2001, **347**: 373
- 12 Suzuki T et al. *Nucl. Phys. A*, 1999, **658**: 313
- 13 Fedorov D V, Jensen A S, Riisager K. *Phys. Rev. C*, 1993, **49**: 201; *Phys. Rev. C*, 1994, **50**: 2372; *Phys. Rev. C*, 1995, **51**: 3052; *Phys. Rev. C*, 1997, **55**: 1327
- 14 Cobis A, Fedorov D V, Jensen A S. *Phys. Rev. C*, 1998, **58**: 1403
- 15 Garrido E, Fedorov D V, Jensen A S. *Phys. Rev. C*, 2003, **68**: 014002
- 16 Zhukov M V, Korshennikov A A, Smedberg M H. *Phys. Rev. C*, 1994, **50**: R1
- 17 Vary J P, Dover C B. *Phys. Rev. Lett.*, 1973, **31**: 1512
- 18 PANG D Y, YE Yan-Lin et al. *AIP Conf. Proc.*, 2006, **865**: 16
- 19 GE Yu-Cheng, YE Yan-Lin et al. *Chin. Phys. Lett.*, 2003, **20**: 7
- 20 Dover C B, Vary J P. *Phys. Rev. C*, 1975, **11**: 1803
- 21 El-Azab Farid M, Mahmoud Z M M, Hassan G S. *Phys. Rev. C*, 2001, **64**: 014310
- 22 XU Chang, REN Zhong-Zhou. *Phys. Rev. C*, 2006, **73**: R041301
- 23 CHEN B Q, MA Z Y, Grümmer F, Krewald S. *Phys. Lett. B*, 1999, **455**: 13—18
- 24 PEI J C, XU F R, Stevensond P D. *Nucl. Phys. A*, 2005, **765**: 29—38
- 25 LIU Jian-Ye, GUO Wen-Jun, REN Zhong-Zhou, XING Yong-Zhong, ZUO Wen, LEE Xi Guo. *Phys. Lett. B*, 2005, **617**: 24—32
- 26 REN Z Z, Carstoiu F. *HEP & NP*, 1995, **19**: 562 (in Chinese)
- 27 Tanihata I et al. *Phys. Rev. Lett.*, 1985, **55**: 2676
- 28 Tanihata I et al. *Phys. Lett. B*, 1985, **160**: 380
- 29 Al-Khalili J S, Tostevin J A. *Phys. Rev. Lett.*, 1996, **76**: 3903
- 30 Liatard E et al. *Europhys. Lett.*, 1990, **13**: 401
- 31 Hansen P G, Jonson B. *Europhys. Lett.*, 1987, **4**: 409
- 32 Thompson I J, Nunes F M, Banilin B V. *Comput. Phys. Commun.*, 2004, **161**: 87
- 33 Sparenberg J M, Baye D. *Phys. Rev. Lett.*, 1997, **79**: 3802
- 34 Bertsch G F, Borysowicz J, Mcmanus H, Love W G. *Nucl. Phys. A*, 1977, **284**: 399
- 35 Chaudhuri A K. *Nucl. Phys. A*, 1986, **449**: 243; *Nucl. Phys. A*, 1986, **459**: 417
- 36 Khoa Dao T, Satchler G R, Von Oertzen W. *Phys. Rev. C*, 1997, **56**: 954
- 37 Kobos A M, Brown B A, Lindsay R, Satchler G R. *Nucl. Phys. A*, 1984, **425**: 205
- 38 Satchler G R, Love W G. *Phys. Rep.*, 1979, **55**: 183
- 39 Tanihata I et al. *Phys. Lett. B*, 1988, **206**: 592
- 40 Gogny D, Pires P, Tourriel R. *Phys. Lett. B*, 1970, **32**: 591
- 41 Audi G, Wapstrab A H, Thibaulta C. *Nucl. Phys. A*, 2003, **729**: 337
- 42 Glauber R J. *Lectures in Theoretical Physics (Vol. 1)*. New York: InterScience, 1959. 315
- 43 Czyz W, Maximon L C. *Ann. Phys. (N.Y.)*, 1969, **52**: 59
- 44 Karol P J. *Phys. Rev. C*, 1975, **11**: 1203
- 45 Charagi S K, Gupta S K. *Phys. Rev. C*, 1990, **41**: 1610
- 46 Ogawa Y et al. *Nucl. Phys. A*, 1992, **543**: 722
- 47 Ozawa A, Suzuki T, Tanihata I. *Nucl. Phys. A*, 2001, **693**: 32
- 48 Neumaier S R et al. *Nucl. Phys. A*, 2002, **712**: 247
- 49 Tanihata I, Hirata D, Kobayashi T, Shimoura S, Sugimoto K, Toki H. *Phys. Lett. B*, 1992, **289**: 261
- 50 Walecka J D. *Theoretical Nuclear Physics and Subnuclear Physics*. Oxford: Oxford University Press, 1995. 11